Acta Pharmacologica Sinica

www.nature.com/aps

ARTICLE

Discovery and identification of a novel small molecule BCL-2 inhibitor that binds to the BH4 domain

Jing-yi Zhou[1], Rui-rui Yang[2,3,4], Jie Chang[1,2], Jia Song[2,5], Zi-sheng Fan[1,2], Ying-hui Zhang[2,3], Cheng-hao Lu[1,2], Hua-liang Jiang[1,2,3], Ming-yue Zheng[1,2,3] and Su-lin Zhang[2,3]

The B-cell lymphoma 2 (BCL-2) protein family plays a pivotal role in regulating the apoptosis process. BCL-2, as an antiapoptotic protein in this family, mediates apoptosis resistance and is an ideal target for cell death strategies in cancer therapy. Traditional treatment modalities target BCL-2 by occupying the hydrophobic pocket formed by BCL-2 homology (BH) domains 1–3, while in recent years, the BH4 domain of BCL-2 has also been considered an attractive novel target. Herein, we describe the discovery and identification of DC-B01, a novel BCL-2 inhibitor targeting the BH4 domain, through virtual screening combined with biophysical and biochemical methods. Our results from surface plasmon resonance and cellular thermal shift assay confirmed that the BH4 domain is responsible for the interaction between BCL-2 and DC-B01. As evidenced by further cell-based experiments, DC-B01 induced cell killing in a BCL-2-dependent manner and triggered apoptosis via the mitochondria-mediated pathway. DC-B01 disrupted the BCL-2/c-Myc interaction and consequently suppressed the transcriptional activity of c-Myc. Moreover, DC-B01 inhibited tumor growth in vivo in a BCL-2-dependent manner. Collectively, these results indicate that DC-B01 is a promising BCL-2 BH4 domain inhibitor with the potential for further development.

Keywords: Bcl-2; BH4 domain; apoptosis; antitumor; virtual screening

Acta Pharmacologica Sinica (2023) 44:475–485; https://doi.org/10.1038/s41401-022-00936-0

INTRODUCTION

Apoptosis is a conserved process regulated by the BCL-2 protein family through its proapoptotic (for example, BAX, BAK, BAD, BIM and PUMA) and antiapoptotic (BCL-2, BCL-XL, MCL-1, BCL-W and BFL-1) members [1–4]. Shifting the balance toward antiapoptotic proteins can lead to apoptosis resistance, which is a hallmark of cancer [5].

BCL-2, as an antiapoptotic protein, contains a transmembrane domain and BH1-BH4 domains, and its BH1-BH3 domains together form a hydrophobic pocket, within which the proapoptotic BCL-2 family members can interact by inserting their BH3 domains [6]. During the past few decades, several BH3 mimetics have been developed to inhibit BCL-2 and induce apoptosis by occupying this hydrophobic pocket [7–14] (Fig. 1a). ABT-737 was first reported as a potent BCL-2 inhibitor that can exert single-agent antitumor activity in animal models as well as primary patient-derived samples [12]. Later, navitoclax (ABT-263) was reported as an analog of ABT-737, which showed an antitumor effect after oral administration [14, 15]; however, it was found to trigger thrombocytopenia due to its inhibition of BCL-XL [16]. Re-engineering navitoclax led to the advent of venetoclax (ABT-199), which showed high selectivity for BCL-2 and particularly low binding affinity toward BCL-XL [13]. Venetoclax is the first approved BCL-2 inhibitor for the treatment of chronic lymphocytic leukemia and acute myeloid leukemia without thrombocytopenia [13]. S55746 was also reported to be orally active and can suppress hematological tumor growth [8]. In addition, APG-2575 showed synthetic lethal effects when used in combination with BTK or MDM2 inhibitors in diffuse large B-cell lymphoma, and it is now being tested in phase I clinical trials [11].

In recent years, with the emerging understanding of BCL-2, its BH4 domain has also been identified as an attractive novel target. The BH4 domain is separated from the hydrophobic groove formed by the BH1-3 domains [17]. Unlike the BH3 domain, which mediates antiapoptotic functions by modulating its interactions with other proapoptotic members of the BCL-2 protein family, the BH4 domain can interact with various apoptosis regulatory proteins beyond BCL-2 family members, such as IP_3R (inositol 1,4,5-trisphosphate receptor) [18], c-Myc [19], Ras [20], Raf-1 [21] and VDAC (voltage-dependent anion channel) [22]. In addition, caspase-mediated cleavage of the BH4 domain can convert BCL-2 from a survival factor into a proapoptotic protein [23]. These facts make it conceivable that the BH4 domain is pivotal for determining the antiapoptotic potential of BCL-2. Furthermore, BDA-366 (Fig. 1b) has been

[1]School of Chinese Materia Medica, Nanjing University of Chinese Medicine, 138 Xianlin Road, Nanjing 210023, China; [2]Drug Discovery and Design Center, State Key Laboratory of Drug Research, Shanghai Institute of Materia Medica, Chinese Academy of Sciences, 555 Zuchongzhi Road, Shanghai 201203, China; [3]University of Chinese Academy of Sciences, No. 19 A Yuquan Road, Beijing 100049, China; [4]Shanghai Institute for Advanced Immunochemical Studies, and School of Life Science and Technology, ShanghaiTech University, 393 Huaxiazhong Road, Shanghai 200031, China and [5]The First Affiliated Hospital of USTC, Division of Life Sciences and Medicine, University of Science and Technology of China, Hefei 230001, China

Correspondence: Hua-liang Jiang (hljiang@simm.ac.cn) or Ming-yue Zheng (myzheng@simm.ac.cn) or Su-lin Zhang (slzhang@simm.ac.cn)

These authors contributed equally: Jing-yi Zhou, Rui-rui Yang

Received: 6 February 2022 Accepted: 2 June 2022
Published online: 2 August 2022

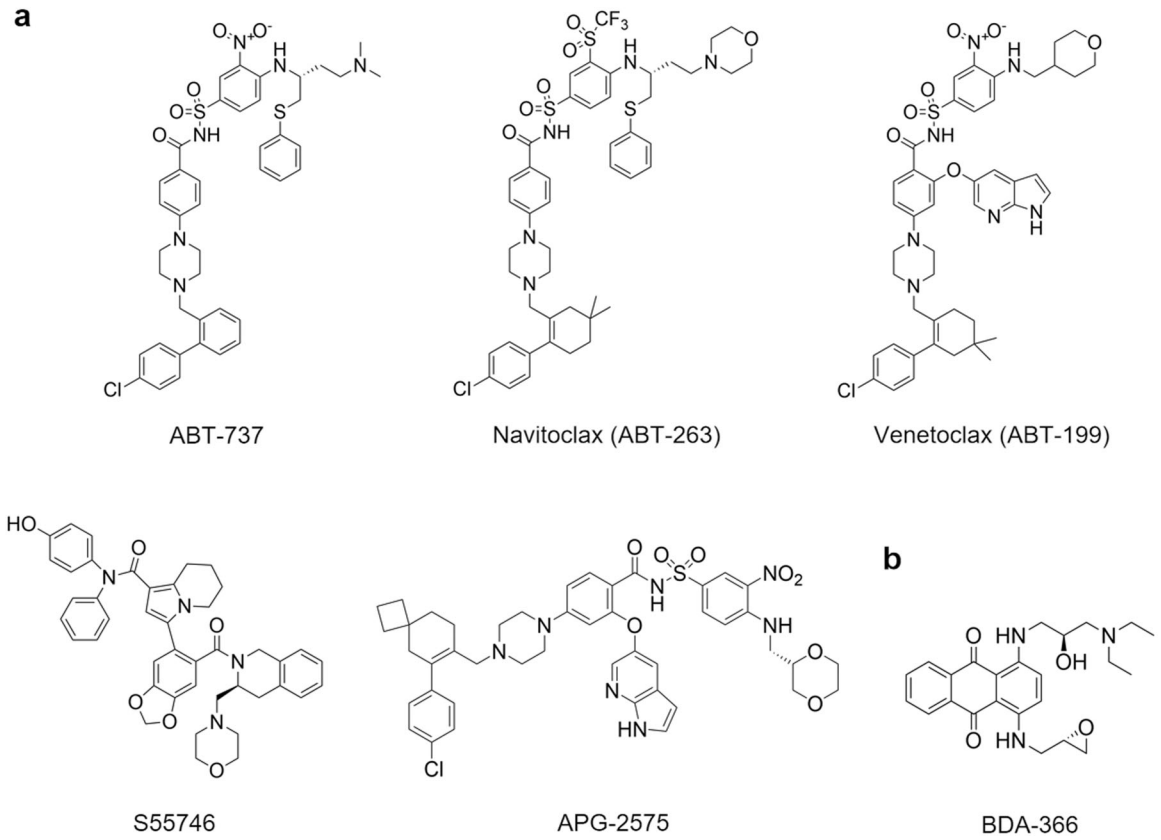

Fig. 1 Reported BCL-2 inhibitors. a Representative BH3 mimetics targeting the hydrophobic binding pocket of BCL-2. **b** BDA-366, a small molecule compound targeting the BCL-2 BH4 domain.

reported to target the BH4 domain of BCL-2 and exhibit strong efficacy against human lung cancer, as evidenced by in vitro experiments as well as in vivo validations [24]. This provides a proof-of-concept supporting the feasibility of a novel strategy targeting the BCL-2 BH4 domain for anticancer therapy. To the best of our knowledge, apart from BDA-366, no other BCL-2 BH4 domain inhibitors have been reported. Therefore, it is still necessary to develop more selective BCL-2 BH4 domain inhibitors for the exploration of BH4 domain function and alternative strategies for cancer therapy.

Herein, we describe the discovery and validation of DC-B01 as a selective BCL-2 BH4 domain inhibitor by combining docking-based virtual screening with biochemical evaluation methods. DC-B01 significantly triggered apoptosis and exhibited a suppressive effect on tumor growth in a BCL-2-dependent manner, suggesting that it is a promising BCL-2 BH4 domain inhibitor with the potential for further development.

MATERIALS AND METHODS

Binding site evaluation by SiteMap

First, the Protein Preparation Wizard module in Maestro software from Schrödinger (2010) was used with the default parameters to prepare the protein structure (1G5M) of BCL-2. Then, the SiteMap module of Maestro was used with the default parameters to evaluate the potential binding sites.

Molecular docking-based virtual screening

A total of 20,000 compounds from our in-house library were screened. The three-dimensional coordinates of these compounds were generated with the LigPrep model of Maestro in default mode. The resulting structures were used for docking. The receptor grid file of BCL-2 was generated using the Glide model. Docking was conducted using Glide software with standard precision mode, followed by redocking of the top poses with extra precision mode.

Plasmid construction and protein purification

The sequences encoding human BCL-2 and its BH3 and BH4 domain deletion mutants were cloned into expression vectors (pET-28a with an N-terminal 6× His tag or pcDNA3.1(+) with an N-terminal Flag tag). For protein purification, the pET-28a vectors were transformed into an *E. coli* strain and cultured in LB medium containing kanamycin at 37 °C. The cells were induced using IPTG (1 mM) overnight at 18 °C. Cell pellets were collected and lysed by sonification in buffer (20 mM HEPES, pH 8.0, 150 mM NaCl, 10 mM imidazole, 1 mM TCEP). The clarified lysates were subjected to purification using Histrap HP columns (GE Healthcare). Further purification was conducted using a Superdex 75 Increase column (GE Healthcare) in BCL-2 buffer (20 mM HEPES, pH 8.0, 300 mM NaCl). Finally, proteins were collected, concentrated, and aliquoted and stored at −80 °C. An Äkta chromatography system was used for all described purification procedures.

Fluorescence polarization (FP) assay

For the primary screening of virtually screened compounds, an FP assay was performed according to a previously described method [24, 25]. The FAM-labeled Bad peptide (5'-FAM-AAAAAQRY-GRELRRMSDEFVDSFKK-3') was synthesized and used as the probe. Briefly, the assay was performed in black 384-well microplates (Corning, 3575) under the following conditions: each individual well contained 5% (*v*/*v*) DMSO, 60 nM FAM-Bad, and 120 nM BCL-2 protein in buffer (20 mM HEPES, pH 8.0, 150 mM NaCl). After incubation at room temperature (RT) for 30 min, the FP values were measured with a Tecan Spark multifunctional microplate reader at 485/535 nm.

A DNA intercalation study was conducted to measure small molecule/DNA binding [26, 27]. The assay was performed in black 384-well microplates (Corning, 3575) under the following conditions: each individual well contained 5% (*v*/*v*) DMSO, 50 nM acridine orange (Sigma, A9231), and 12.5 μg · mL^{-1} HT-DNA (Sigma, D6898-10G) in HEN buffer (10 mM HEPES, 1 mM EDTA, pH 7.5, 100 mM NaCl). After incubation (RT, 30 min), the FP values were measured with a Tecan Spark multifunctional microplate reader at 485/535 nm.

Pan-assay interference compound test

To test whether the compound is intrinsically fluorescent, DC-B01 was serially diluted in buffer (20 mM HEPES, pH 7.4), and the fluorescence intensity was measured at 485/535 nm.

Fluorescence polarization and homogeneous time-resolved fluorescence (HTRF) assays were then conducted for further validation. FP validation performed on STING was conducted in an assay system containing serially diluted compounds, 125 nM tracer (Cy5-GSK-3) [28, 29] and 625 nM STING in buffer (20 mM HEPES, pH 7.4). For SPOP, FP validation was conducted in an assay system containing serially diluted compounds, 100 nM SPOP and 100 nM probe (FITC-LACDEVTSTTSSSTA) [30, 31] in buffer (20 mM HEPES, pH 7.4). Black 384-well microplates (Corning, 3575) were used for the FP assay, and the FP values were measured after incubation (RT, 30 min). HTRF validation performed on KRAS-G12D was conducted in a white Opaque 384-well microplate (PerkinElmer). First, 10 nM GST-tagged KRAS-G12D together with anti-GST Tb (Cisbio) were incubated with compounds for 15 min at RT, and a mixture of 100 nM his-SOS1 and 100 nM Cy5-GTP was added. After further incubation at RT for 30 min, HTRF was measured.

Surface plasmon resonance (SPR)

We investigated the ability of compounds to bind to proteins with an SPR assay conducted on a Biacore T200 instrument (GE Healthcare). The purified proteins were immobilized onto CM5 sensor chips, and compounds in a series of twofold dilutions were flowed through the sensor chip at 30 μL · min^{-1}. The K_D values were derived using Biacore T200 Evaluation software (GE Healthcare).

Cell culture

The cell lines DB, NCI-H460, A375, MDA-MB-231, Caki-2 and HEK293 were obtained from the Cell Bank of the Chinese Academy of Sciences and Cell Resource Center of Peking Union Medical College; RS4;11 was purchased from ATCC (American Type Culture Collection). DB, H460 and RS4;11 cells were cultured in RPMI-1640 medium (BasalMedia, L210KJ); A375, MDA-MB-231 and HEK293 cells were cultured in DMEM (BasalMedia, L110KJ); and Caki-2 cells were cultured in McCoy's 5 A medium (BasalMedia, L630KJ). Additionally, 10% FBS (Gibco, 10099141 C) and 1% penicillin-streptomycin (Gibco, 2321118) were added to all culture media. Cells were cultured at 37 °C under a humidified, 5% (*v*/*v*) CO_2-containing atmosphere.

Cell viability assay

Cell viability was measured using CellTiter-Glo® Reagent (Promega, G7570) as previously described [8].

Western blot

Cell lysates containing equal amounts of protein were denatured, subjected to electrophoresis on SDS-PAGE gels, and transferred onto nitrocellulose membranes. The blots were blocked with 5% skim milk and then incubated at 4 °C overnight with the corresponding primary antibodies against BCL-2 (4223), MCL-1 (39224), BCL-XL (2764), cytochrome *c* (11940), β-tubulin (15115), GAPDH (5174), DYKDDDK Tag (14793), c-Myc (18583) and cleaved caspase-3 (9664), which were purchased from Cell Signaling Technology. After incubation with the secondary antibody (Promega, W4011) for 1.5 h at RT, the bands on the membranes were visualized using an ECL kit (Meilun, MA0186) and GENESys V1.6.6.0.

Cellular thermal shift assay (CETSA)

HEK293 cells were harvested after transfection with the indicated Flag-tagged plasmids for 24 h. Cell lysates were collected and divided into two equal portions. Before being aliquoted into PCR tubes, the lysates were mixed with 100 μM DC-B01 and the same volume of DMSO. After incubation (RT, 30 min), the samples were subjected to CETSA heating at a pre-established temperature gradient for 3 min. The soluble components were then analyzed by Western blot.

Mitochondrial cytochrome *c* release assay

Cells were harvested and processed for subcellular fractionation using the Cell Mitochondria Isolation Kit (Beyotime, C3601) following the manufacturer's protocol. The samples containing mitochondrial or cytosolic proteins were collected for further western blot analysis.

Knockdown of *BCL-2*

BCL-2 shRNA lentivirus was obtained from the commercial source Genomeditech. Cells were infected with *BCL-2* shRNA lentivirus and grown in complete medium containing 5 μg ml^{-1} puromycin.

Flow cytometry analysis

Cell apoptosis was evaluated using the Annexin V-FITC/PI Apoptosis Detection Kit (Vazyme Biotech, A211-01), and mitochondrial membrane potential (MMP) depolarization was detected using the JC-1 assay kit (Beyotime, C2006). Samples were analyzed using a CytoFlex flow cytometer (Beckman).

Coimmunoprecipitation (Co-IP)

DB and H460 cells were harvested after 24 h of treatment with DC-B01 and lysed on ice in cell lysis buffer (Beyotime, P0013) containing protease inhibitor (Bimake, B15001). The clarified cell lysates were immunoprecipitated with Protein A/G MagBeads (GenScript, L00277) combined with a c-Myc antibody (Cell Signaling Technology, 18583) overnight at 4 °C. The beads were washed at least 3 times using PBST before being analyzed by SDS-PAGE.

Real-time quantitative PCR (RT-qPCR)

RNA-easy Isolation Reagent (Vazyme, R701-01) was used to extract total RNA, and HiScript III qRT SuperMix (Vazyme, R323-01-AC) was used to synthesize cDNA. RT-qPCR was conducted in a Bio-Rad CFX96 RealTime PCR Detection System using ChamQ SYBR qPCR Master Mix (Vazyme, Q331-AA). The primer sequences used in this experiment were as follows: human *LDHA* forward: 5'-GGCTACAA CAGGATTCTA-3'; human *LDHA* reverse: 5'-TTACAAACCATTCTTA TTTCTAAC-3'; human *CDK4* forward: 5'-GGTAGTGGAAAACCAG-CAGCC-3'; human *CDK4* reverse: 5'-TAGAAATACGGCTGCACCGAG-3'; human *c-Myc* forward: 5'-GGTAGTGGAAAACCAGCAGCC-3'; human *c-Myc* reverse: 5'-TAGAAATACGGCTGCACCGAG-3'; and human *ACTB* forward: 5'-CATGTACGTTGCTATCCAGGC-3'; human *ACTB* reverse: 5'-CTCCTTAATGTCACGCACGAT-3'.

In vivo treatment of xenografts with DC-B01

All procedures performed on animals were approved by the Institutional Animal Care and Use Committees of Shanghai Institute of Materia Medica, Chinese Academy of Sciences (IACUC Issue NO. 2021-10-JHL-24). BALB/c nude mice (female) were obtained from Beijing Huafukang Biotechnology and subcutaneously inoculated with H460 cells (5×10^6 cells per mouse) or *BCL-2*-knockdown H460 cells (1×10^7 cells per mouse). When the tumor volume reached ~100 mm^3, the mice were randomly divided into treatment (15 mg/kg per day) and vehicle control

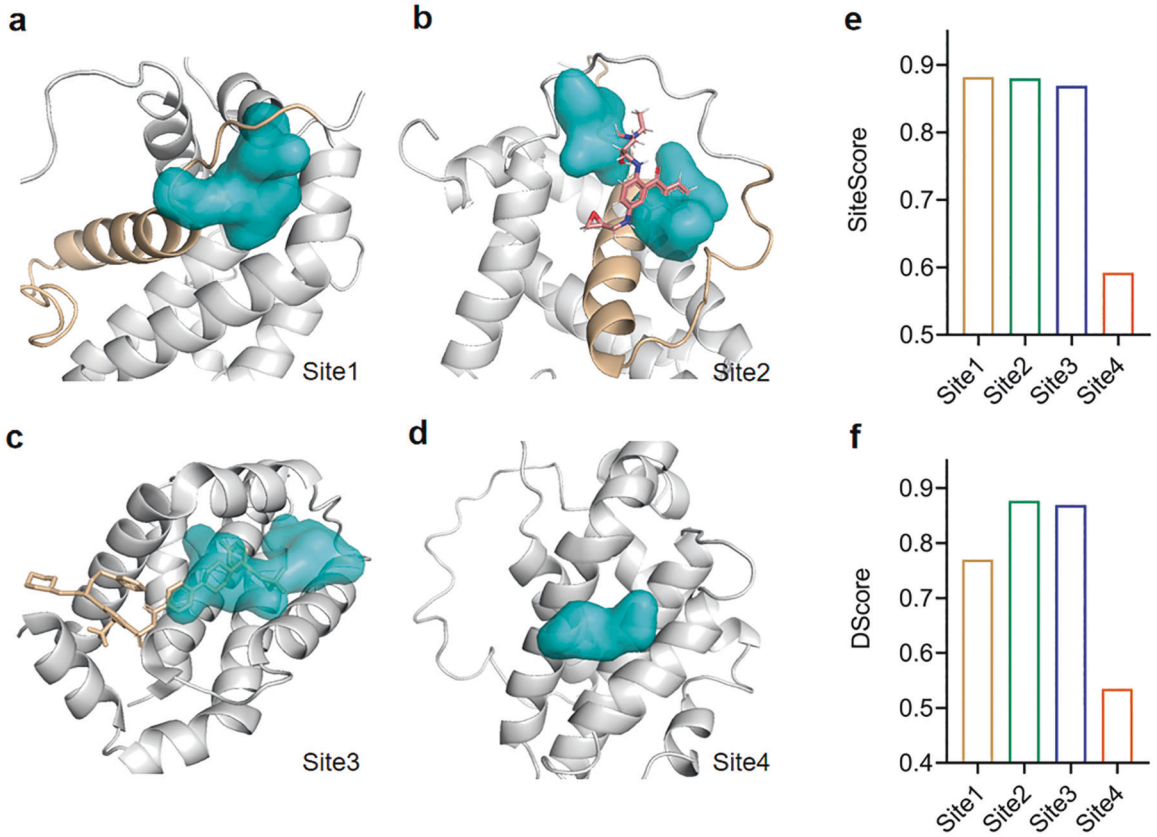

Fig. 2 Evaluation of the potential binding sites of BCL-2. a–d Potential BCL-2 binding sites (colored cyan) generated by Schrödinger SiteMap. Site 1 (**a**) and site 2 (**b**) are located near the BH4 domain (presented in light orange), and site 3 (**c**) is located near the BH3 domain, which is the binding site for navitoclax (presented in light orange). **e**, **f** The SiteScores (**e**) and DScores (**f**) of all four sites.

($n = 6$) groups. DC-B01 was formulated for intraperitoneal injection in 25% polyethylene glycol (PEG) 400, 70% PBS and 5% DMSO. Tumor length, tumor width and mouse body weight were recorded every day, and the tumor volume was calculated from the following equation: $V = (\text{length} \times \text{width}^2)/2$. At the end of this study, the mice were euthanized, and the tumors were harvested.

Statistical analysis

GraphPad Prism 8.0 was used to perform statistical analysis. All numerical results are displayed as the mean ± SD. Differences between groups were determined using a 2-tailed unpaired *t* test. The significance levels were set as $^{*}P < 0.05$; $^{**}P < 0.01$, $^{***}P < 0.001$.

RESULTS

Evaluation of the small molecule binding sites of the BCL-2 BH4 domain

To discover selective BCL-2 BH4 inhibitors, Schrödinger SiteMap was utilized to seek and evaluate potential binding sites of BCL-2. Four potential BCL-2 binding sites were generated, and sites 1–3 had SiteScores greater than 0.8 (Fig. 2a-e), indicating that these three sites are probable compound binding sites [32–34]. Among them, site 3 is located near the BH3 domain, which is the exact binding site for BH3 mimetics such as navitoclax [13], suggesting that it is feasible to use Schrödinger SiteMap to discover potential BCL-2 binding sites. Both site 1 and site 2 are located near the BH4 domain, whereas site 2 showed a higher DScore, which is used to predict the druggability of binding sites [33] (Fig. 2f). We next compared the binding site of BDA-366 [24] to predicted site 2 of BCL-2 and found that former is located at the bottom to the right inside site 2 and is a part of site 2 (Fig. 2b). This result suggests that it is more likely to discover BH4 domain inhibitors using predicted site 2 rather than the BDA-366 binding site. Accordingly, site 2 was chosen as the most promising binding site near the BH4 domain and was employed in subsequent structure-based virtual screening for the discovery of selective BCL-2 BH4 domain inhibitors.

Discovery and validation of small molecules targeting the BCL-2 BH4 domain binding site via biochemical and biophysical assays

The overall workflow to find small molecules targeting the BCL-2 BH4 domain is shown in Fig. 3a. A total of 20,000 compounds from our in-house library were docked into the site 2 pocket (Fig. 2b). The top-ranked 5,000 poses were clustered into 60 groups, and 50 compounds were selected based on their physicochemical properties. Then, a fluorescence polarization (FP) assay was performed to measure the ability of the small molecules to inhibit BCL-2 binding to its substrate, peptide Bad, in vitro. Among these 50 candidates, DC-B01 was identified as an inhibitor capable of competing with a fluorescent Bad peptide (5'-FAM-AAAAAQRYGRELRRMSDEFVDSFKK-3') for binding to BCL-2 with an IC_{50} value of 4.75 μM (Fig. 3b, c). We searched for DC-B01 and its derivatives on SciFinder (https://scifinder.cas.org), but no related biological activities of DC-B01 or its derivatives with greater than 80% similarity had been previously reported.

We next sought to identify whether DC-B01 could directly bind to the BH4 domain of BCL-2. To this end, BH3 domain deletion (ΔBH3) and BH4 domain deletion (ΔBH4) mutant BCL-2 proteins were purified. We first tested whether DC-B01 could directly target the BCL-2 BH4 domain using a surface plasmon resonance (SPR) assay. DC-B01 exhibited micromolar binding affinity to both the full-length and ΔBH3 BCL-2 protein with an estimated K_D value of

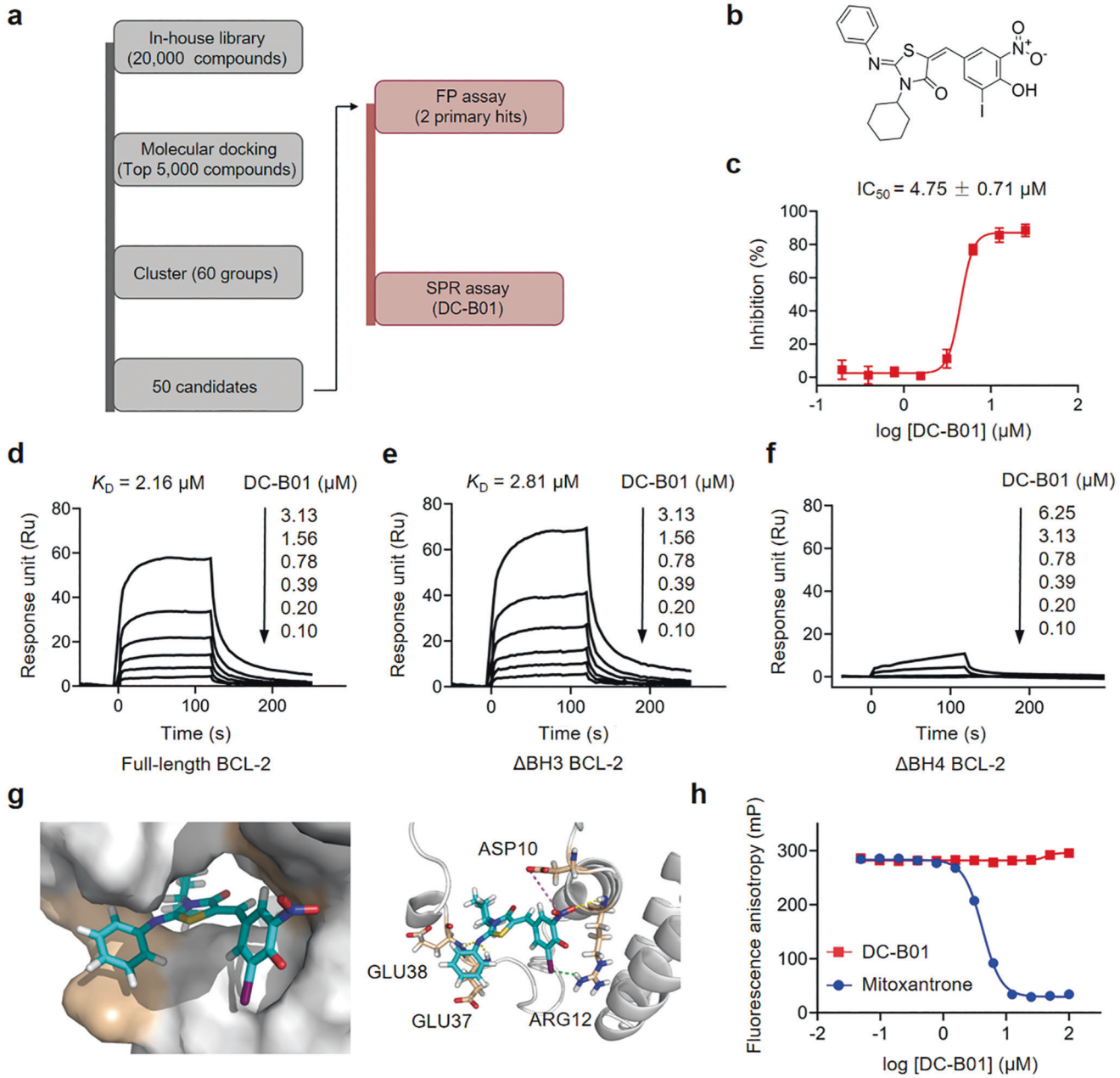

Fig. 3 Discovery and validation of DC-B01 as a selective inhibitor of the BCL-2 BH4 domain. a Overview of the screening procedure for BCL-2 BH4 domain inhibitors. **b** Chemical structure of DC-B01. **c** The IC_{50} value of DC-B01 competitively inhibiting the peptide Bad from binding to BCL-2 as measured by FP assay. **d**–**f** SPR binding curves for different concentrations of DC-B01 binding to full-length BCL-2 (**d**), ΔBH3 BCL-2 (**e**), and ΔBH4 BCL-2 (**f**). **g** The putative binding mode of DC-B01 to the BCL-2 BH4 domain. The residues that interact with DC-B01 are highlighted in stick format. The hydrogen bonds and halogen bond are presented as yellow and green dashes, respectively, and the salt bridge is presented in pink. **h** DC-B01 was tested in an FP assay for its ability to bind to DNA and compared with mitoxantrone, a known DNA intercalator. Data are shown as the mean ± SD of at least three independent experiments.

2.16 μM and 2.81 μM, respectively (Fig. 3d, e), whereas DC-B01 exhibited much weaker binding affinity to ΔBH4 BCL-2 protein (Fig. 3f), suggesting that DC-B01 preferred to bind with the BH4 domain rather than the BH3 domain of BCL-2.

To further confirm the interaction between DC-B01 and the BCL-2 BH4 domain, we performed a cellular thermal shift assay (CETSA) in HEK293 cells transfected with full-length BCL-2 or its truncated mutants. The results revealed that treatment with DC-B01 increased the thermal stability of the full-length and ΔBH3 BCL-2 proteins but not the ΔBH4 BCL-2 protein (Supplementary Fig. 1a-c), suggesting that DC-B01 selectively binds to the BH4 domain rather than the BH3 domain.

To gain structural insight into the interaction between DC-B01 and the BH4 domain of BCL-2, we docked DC-B01 into the site 2 pocket of BCL-2 (PDB ID: 1G5M). As shown in Fig. 3g, DC-B01 was embedded in the pocket consisting of the helix and loop of the BH4 domain. DC-B01 can form three hydrogen bonds with ARG12, GLU37 and GLU38, a halogen bond with ARG12, and a salt bridge between its nitryl group and ASP10 in the binding pocket. The docking pose and these key interactions provided proof that DC-B01 directly binds to the BH4 domain of BCL-2.

To determine whether DC-B01 reacts with DNA as a crosslinker, we performed another FP assay to validate its capacity to intercalate DNA. By comparison with mitoxantrone, a known

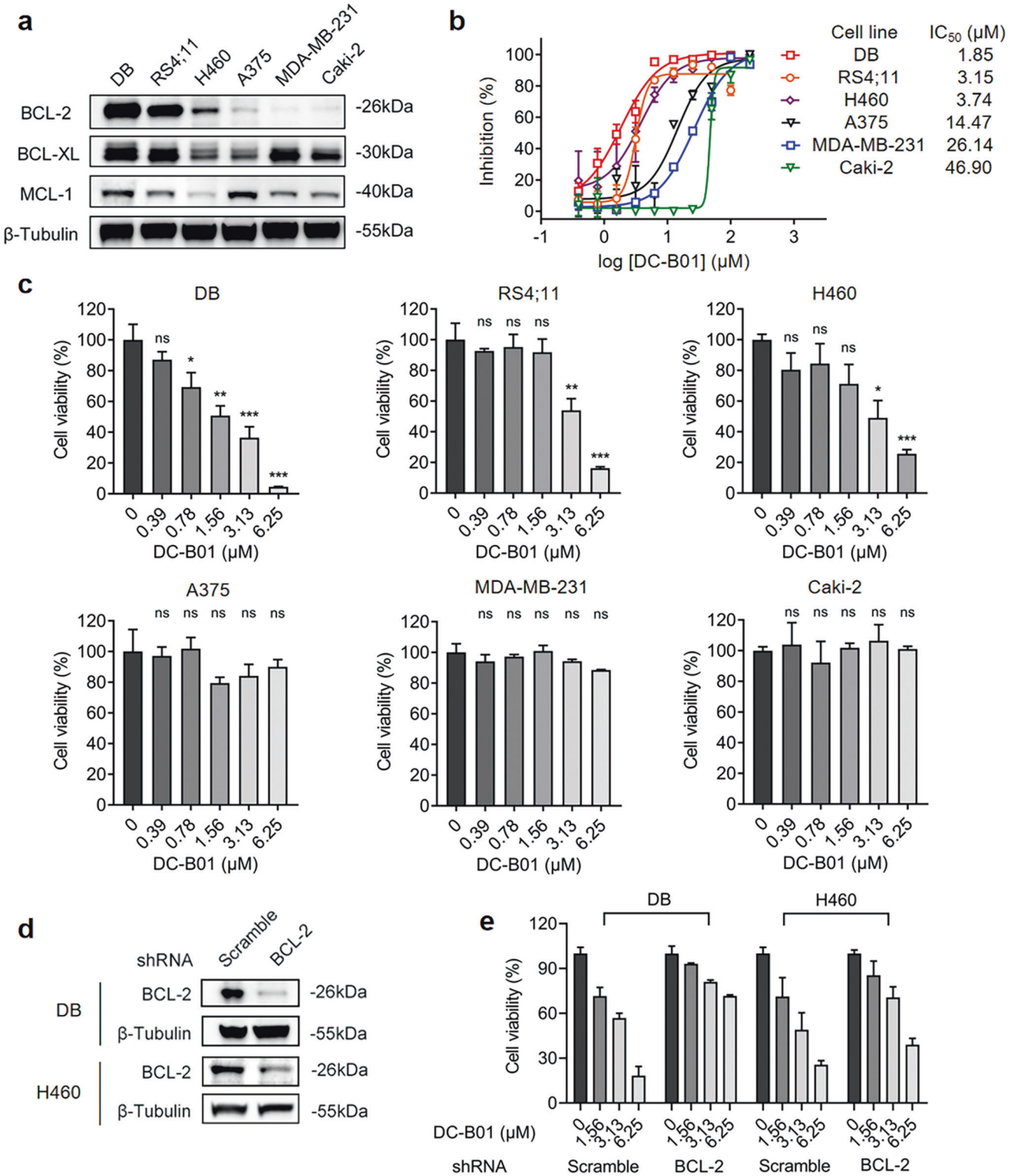

Fig. 4 DC-B01 induces cancer cell killing in a BCL-2-dependent manner. a Expression of the endogenous proteins BCL-2, BCL-XL and MCL-1 in the indicated cancer cell lines. **b**, **c** Viability of cancer cells treated with increasing concentrations of DC-B01 for 72 h. **d** Western blots showing BCL-2 expression in DB and H460 cells infected with scramble or *BCL-2* shRNA lentivirus. **e** Viability of DB and H460 cells after treatment with DC-B01 for 72 h. Data are shown as the mean ± SD of at least three independent experiments. $^{*}P < 0.05$; $^{**}P < 0.01$; $^{***}P < 0.001$ vs. control.

DNA intercalator, DC-B01 was determined to not bind to DNA (Fig. 3h), which helps to rule out the possibility that DC-B01 is a DNA binding agent that triggers apoptosis. In addition, we conducted further experiments to rule out the possibility that DC-B01 is a pan-assay interference compound. DC-B01 is not intrinsically fluorescent (Supplementary Fig. 2a). To eliminate possible effects caused by aggregation, we measured and compared the activity of DC-B01 through a FP assay in buffer with or without the surfactant Tween 20, and no significant change in IC_{50} value was observed (Supplementary Fig. 2b) after adding

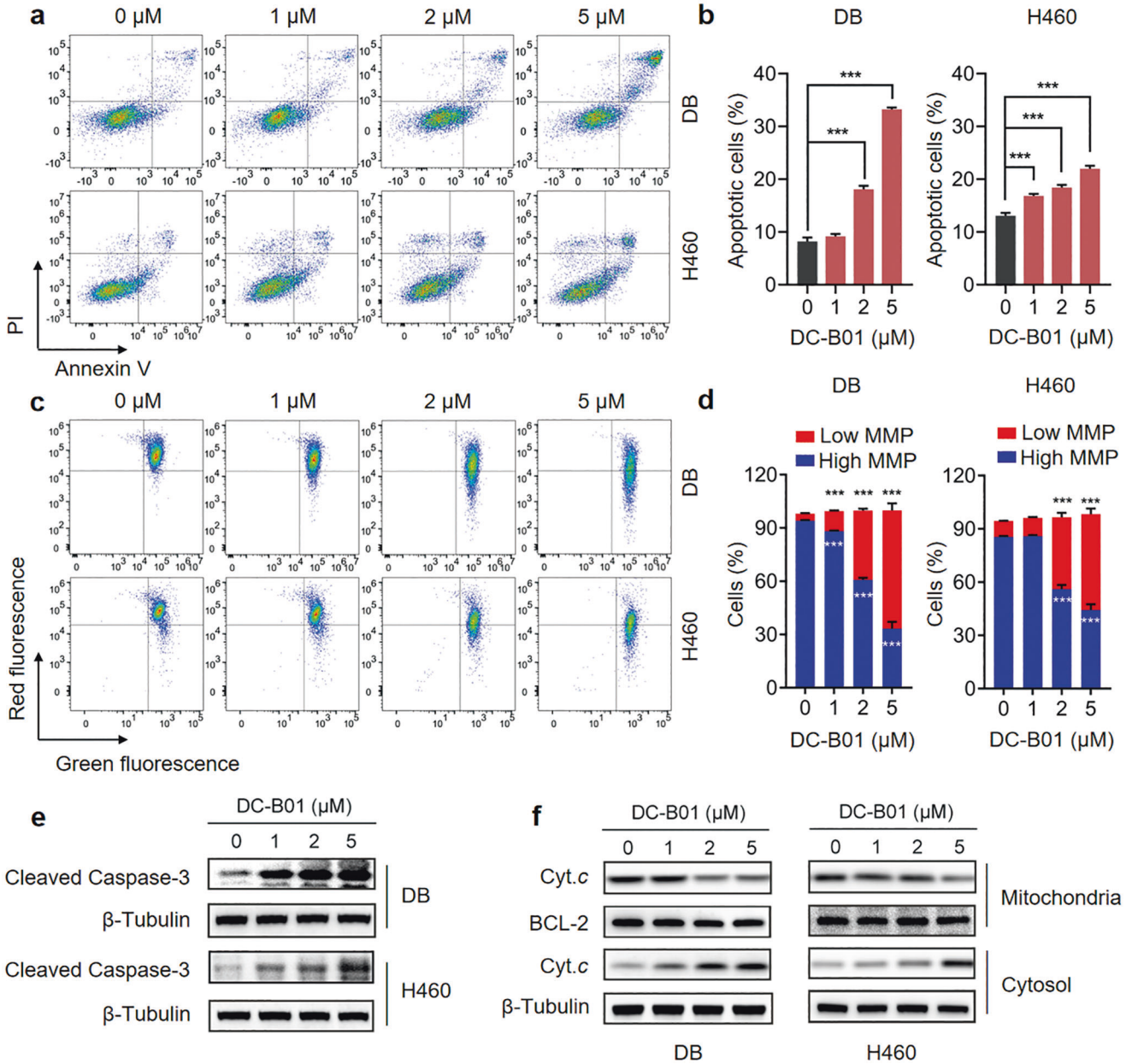

Fig. 5 DC-B01 induces apoptosis via the mitochondria-mediated apoptosis pathway. a, **b** Annexin V and PI double-staining to evaluate cell apoptosis induced by DC-B01 (0, 1, 2, 5 μM, 24 h) in DB and H460 cells (**a**). The percentages of apoptotic DB cells and H460 cells were quantified (**b**). **c, d** Changes in MMP induced by DC-B01 (0, 1, 2, 5 μM, 24 h) in DB and H460 cells measured by flow cytometric analysis (**c**). The percentages of high MMP and low MMP were quantified (**d**). **e** Western blot analysis evaluated the change in cleaved caspase-3 expression in DB and H460 cells after treatment with DC-B01 (0, 1, 2, 5 μM, 24 h). **f** Western blots showing the concentrations of mitochondrial and cytosolic cytochrome *c* in DB and H460 cells after treatment with DC-B01 (0, 1, 2, 5 μM, 4 h). BCL-2 and β-tubulin served as the loading controls. Data are shown as the mean ± SD of at least three independent experiments. ***$P < 0.001$ vs. control.

surfactant to the assay buffer (20 mM HEPES, pH 8.0, 150 mM NaCl, 0.05% Tween 20). To complement this result, we analyzed the fluorescent character of DC-B01 and tested its activity in different screening systems with different proteins. Compared with the positive controls, DC-B01 showed no significant binding to these other proteins, including $KRAS^{G12D}$, SPOP, and STING (Supplementary Fig. 2c-e). These data indicated that DC-B01 does not behave as a pan-assay interfering compound.

DC-B01 induces cancer cell killing in a BCL-2-dependent manner
To investigate the effect of DC-B01 on cancer cell killing and determine whether the cell killing response is dependent on the expression levels of endogenous BCL-2, six cancer cell lines expressing relatively higher, relatively lower or undetectable levels of endogenous BCL-2 were selected to measure the growth inhibition effect of DC-B01 (Fig. 4a). DC-B01 significantly inhibited the growth of cancer cells expressing relatively higher levels of BCL-2 (DB, RS4;11, H460) (Fig. 4a–c). In contrast, cancer cells expressing relatively lower or undetectable levels of BCL-2 (A375, MDA-MB-231, Caki-2) were less sensitive to DC-B01 (Fig. 4a–c). Moreover, cell sensitivity to DC-B01 treatment did not appear to be significantly affected by the expression levels of BCL-XL or MCL-1 (Fig. 4a), indicating DC-B01's selectivity for BCL-2 at the cellular level. To further determine the target specificity of DC-B01, we generated stable *BCL-2*-knockdown DB cells and H460 cells using *BCL-2* shRNA lentivirus, and the depletion of BCL-2 was

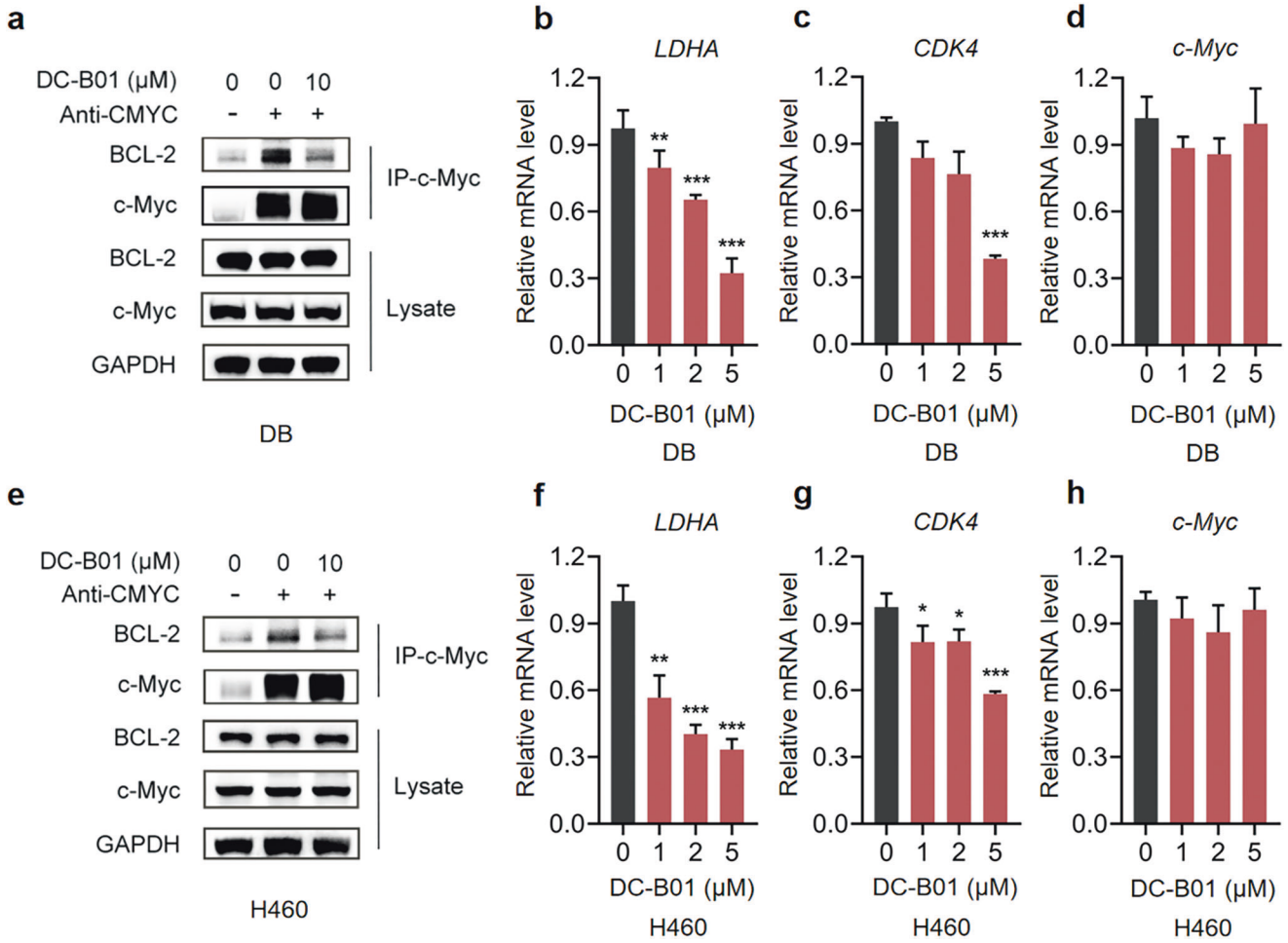

Fig. 6 DC-B01 suppresses the transcriptional activity of c-Myc via inhibition of the BCL-2/c-Myc interaction. a DC-B01 disrupts the BCL-2/c-Myc interaction in DB cells. **b-d** The mRNA expression of *LDHA* (**b**), *CDK4* (**c**) and *c-Myc* (**d**) was detected in DB cells at 24 h by RT-qPCR. **e** DC-B01 disrupts the BCL-2/c-Myc interaction in H460 cells. **f-h** The mRNA expression of *LDHA* (**f**), *CDK4* (**g**) and *c-Myc* (**h**) was detected in H460 cells at 24 h by RT-qPCR. Data are shown as the mean ± SD of at least three independent experiments. $^{*}P < 0.05$; $^{**}P < 0.01$; $^{***}P < 0.001$ vs. control.

verified by Western blot (Fig. 4d). BCL-2 depletion led to resistance to DC-B01 treatment (Fig. 4e), suggesting a direct correlation between the BCL-2 expression level and sensitivity to DC-B01. Taken together, these results revealed that DC-B01 induces cancer cell killing in a BCL-2-dependent manner.

DC-B01 induces apoptosis via the mitochondria-mediated apoptosis pathway

We next sought to determine whether the cell killing effect induced by DC-B01 was associated with the mitochondrial apoptotic pathway. We first evaluated whether DC-B01 could induce apoptosis in cancer cells by flow cytometry. As indicated by the externalization of phosphatidylserine detected by Annexin V-FITC/PI staining, DC-B01 triggered apoptosis in DB and H460 cells in a dose-dependent manner (Fig. 5a, b). In addition, we measured the mitochondrial membrane potential (MMP) using JC-1 staining, as MMP depolarization is a hallmark event in the mitochondrial apoptotic pathway [35]. In healthy cells, JC-1 can aggregate and exhibit red fluorescence signals in mitochondria with a high MMP, while in apoptotic cells, the MMP decreases, which converts JC-1 from an aggregated state to a monomeric state, exhibiting green fluorescence signals. As expected, the MMP was markedly decreased after DC-B01 treatment, as indicated by the weakened JC-1 red fluorescence representing the loss in MMP (Fig. 5c, d) in DB and H460 cells. Consistent with the above results, we further observed significant enhancement in caspase-3 activity (Fig. 5e) and increased release of cytochrome *c* from the mitochondria to the cytosol in a dose-dependent manner in DB and H460 cells after DC-B01 treatment (Fig. 5f). Collectively, these data demonstrate that DC-B01 triggers apoptosis via the mitochondria-mediated apoptosis pathway regulated by BCL-2.

DC-B01 suppresses the transcriptional activity of c-Myc via inhibition of the BCL-2/c-Myc interaction

BCL-2 has been reported to bind directly to c-Myc through its BH4 domain, and through this interaction, BCL-2 can enhance c-Myc transcriptional activity [19]. To test whether DC-B01 inhibits the BCL-2/c-Myc interaction, we conducted coimmunoprecipitation experiments in DB and H460 cells. The results revealed that DC-B01 can disrupt the BCL-2/c-Myc interaction in DB (Fig. 6a) and H460 cells (Fig. 6e). Further RT-qPCR analysis revealed that the mRNA expression levels of *LDHA* and *CDK4*, the target genes of c-Myc, were decreased by treatment with DC-B01 in DB (Fig. 6b, c) and H460 (Fig. 6f, g) cells, yet the expression of *c-Myc* was not significantly affected (Fig. 6d, h). Taken together, these results revealed that DC-B01 suppresses the transcriptional activity of c-Myc via inhibition of the BCL-2/c-Myc interaction.

DC-B01 effectively suppresses tumor growth of H460 lung cancer xenografts in a BCL-2-dependent manner

To investigate the antitumor effect of DC-B01 in vivo, we administered DC-B01 to BALB/c nude mice bearing subcutaneous

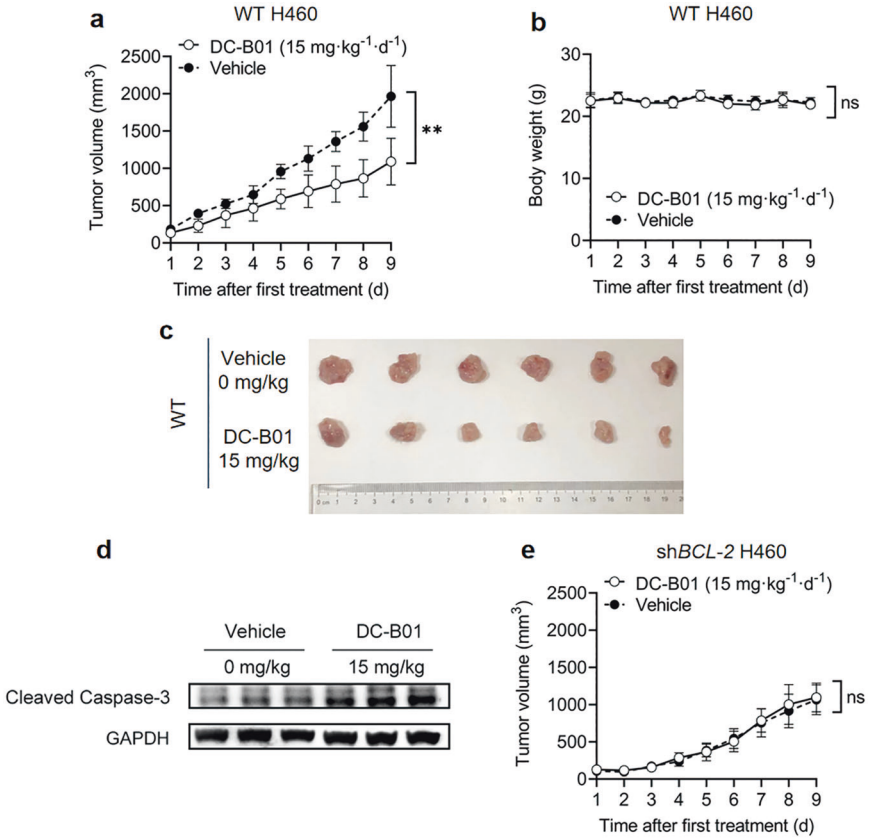

Fig. 7 DC-B01 represses the growth of H460 lung cancer tumor xenografts in a BCL-2-dependent manner. a Volume measurements of H460 xenograft tumors treated with vehicle or DC-B01 for 9 days. **b** Body weight measurements of H460 tumor-bearing mice treated with vehicle or DC-B01. **c** Images of harvested tumors from H460 tumor-bearing mice at Day 9. **d** Western blot analysis of cleaved caspase-3 levels in tumor tissue lysates from three different vehicle- and DC-B01-treated mice. **e** Tumor volume measurements of BALB/c nude mice inoculated with *BCL-2*-knockdown H460 cells. Data are shown as the mean ± SD, $n = 6$. $^{**}P < 0.01$ vs. control.

H460 tumors and monitored tumor growth. The mice were intraperitoneally injected with DC-B01 ($15\ mg \cdot kg^{-1} \cdot d^{-1}$) or vehicle control for 9 days. The suppressive effect of DC-B01 on H460 tumor growth was clearly observed by the tumor volume reduction (TGI = 44.46%) compared with the vehicle group as measured at Day 9 (Fig. 7a, c). To further determine whether the antitumor activity of DC-B01 in the in vivo model is associated with the apoptosis mechanism, we measured the level of cleaved caspase-3 in the tumor tissues by Western blot. As shown in Fig. 7d, the cleaved caspase-3 level in the DC-B01-treated group was significantly higher than that in the vehicle group, indicating that DC-B01 exerts its tumor suppressive effect by inducing apoptosis in H460 lung cancer xenografts.

To explore the role of BCL-2 in DC-B01's antitumor effect, we performed further validation on BALB/c nude mice bearing *BCL-2*-knockdown H460 cell xenografts. As expected, the *BCL-2*-knockdown H460 cell xenografts were resistant to DC-B01 (Fig. 7e), suggesting that the suppressive effect of this compound on tumor growth depends on BCL-2 expression. In addition, no significant body weight loss was observed in the treatment group throughout the 9-day study time (Fig. 7b), indicating the low toxicity of DC-B01 for antitumor efficacy studies at a dose of 15 mg/kg. In summary, these results indicated that DC-B01 induces antitumor effects in a BCL-2-dependent manner in vivo.

DISCUSSION

Overexpression of BCL-2 can lead to apoptosis evasion, which is a main factor contributing to tumor development and has been widely found in diverse cancers, such as lymphoma, leukemia, lung cancer and breast cancer [36–39]. Therefore, targeting BCL-2 is of great significance in cancer therapy. In the past two decades, extensive efforts targeting BCL-2 have contributed to the development of multiple potent BCL-2 inhibitors. These inhibitors disrupt the interaction between BCL-2 and proapoptotic family members by occupying the hydrophobic groove of BCL-2 so that the proapoptotic proteins can carry out their normal functions to kill cancer cells. Among these inhibitors, venetoclax (ABT-199) is the only approved BCL-2 inhibitor, as it has shown high potency and a particularly low number of side effects in clinical trials; it is therefore used in the treatment of several types of lymphocytic leukemia [9]. In recent years, with the emerging understanding of BCL-2, the BH4 domain has been found to be essential for its antiapoptotic function. The BCL-2 BH4 domain is also involved in direct interactions with other apoptosis regulatory proteins beyond the proapoptotic BCL-2 protein family [40]. Therefore, developing small molecules targeting the BH4 domain of BCL-2 has become a new endeavor in recent years. Although theories about targeting the BH4 domain to regulate the antiapoptotic activity of BCL-2 have been proposed, BDA-366 is the only reported molecule targeting the BH4 domain as a proof-of-concept. Therefore, it is urgent to develop additional selective BCL-2 BH4 domain inhibitors.

In this study, starting with Schrödinger SiteMap analysis to identify a promising BCL-2 BH4 domain binding site, followed by docking-based virtual screening and biochemical evaluation, we identified a potential BCL-2 BH4 domain inhibitor, DC-B01. The results from SPR and CETSA confirmed that the BH4 domain rather than the BH3 domain is responsible for the interaction between the BCL-2 protein and DC-B01. Our further study at the cellular

level showed that DC-B01 induces stronger cell killing in cancer cells with higher expression levels of BCL-2, which is similar to previously reported BCL-2 inhibitors [14, 41]. In addition, this killing effect has no distinct correlation with the endogenous expression of BCL-XL or MCL-1, suggesting DC-B01's selectivity for BCL-2. To further determine whether the cell killing effect induced by DC-B01 was associated with apoptosis, we performed flow cytometry and Western blot to detect the specific hallmarks of apoptosis progression. We found that DC-B01 induces cell apoptosis via the BCL-2-regulated mitochondrial pathway, as indicated by the externalization of phosphatidylserine, MMP depolarization, and increased release of cytochrome *c* together with activated caspase-3. As two major oncogenic proteins, BCL-2 can bind directly to c-Myc through its BH4 domain and enhance c-Myc transcriptional activity [19]. Our coimmunoprecipitation study revealed that DC-B01 can disrupt the BCL-2/c-Myc interaction in DB and H460 cells. Furthermore, treatment with DC-B01 decreased the mRNA expression of LDHA and CDK4 with no distinct decline in c-Myc mRNA expression, suggesting that DC-B01 suppresses the transcriptional activity of c-Myc via inhibition of the BCL-2/c-Myc interaction. Additionally, we examined the therapeutic antitumor effect of DC-B01 in BALB/c nude mice bearing H460-transplanted tumors. As expected, DC-B01 caused notable tumor growth inhibition in the H460 lung cancer xenograft model. To further determine whether DC-B01 exerts its therapeutic effect by targeting BCL-2, we used stable *BCL-2*-knockdown H460 cells to establish a transplanted tumor model in BALB/c nude mice. As expected, *BCL-2*-knockdown H460 cell xenografts were resistant to DC-B01 treatment, suggesting that its suppressive effect on tumor growth is BCL-2 dependent.

In summary, we discovered and identified DC-B01 as a novel small molecule inhibitor of BCL-2 that selectively binds to the BH4 domain and confirmed its antitumor effects in vitro and in vivo. All of the experimental data revealed that DC-B01 is a potential candidate that targets the BCL-2 BH4 domain and possesses the potential for further development.

ACKNOWLEDGEMENTS

This work was supported by the Lingang Laboratory (LG202102-01-02; LG-QS-202204-01), the National Natural Science Foundation of China (81903639), the Shanghai Municipal Science and Technology Major Project, the Natural Science Foundation of Shanghai (22ZR1474300) and the Shanghai Sailing Program (19YF1457800).

AUTHOR CONTRIBUTIONS

MYZ and SLZ designed the research. MYZ, SLZ, and HLJ supervised the study. JYZ and RRY developed the methodology. JYZ, RRY, JC, JS, ZSF, YHZ, and CHL acquired and analyzed the data. SLZ, JYZ, RRY, and JC wrote and reviewed the manuscript. All authors discussed the study.

ADDITIONAL INFORMATION

Supplementary information The online version contains supplementary material available at https://doi.org/10.1038/s41401-022-00936-0.

Competing interests: The authors declare no competing interests.

REFERENCES

1. Chipuk JE, Moldoveanu T, Llambi F, Parsons MJ, Green DR. The BCL-2 family reunion. Mol Cell. 2010;37:299–310.
2. Czabotar PE, Lessene G, Strasser A, Adams JM. Control of apoptosis by the BCL-2 protein family: Implications for physiology and therapy. Nat Rev Mol Cell Biol. 2014;15:49–63.
3. Shamas-Din A, Brahmbhatt H, Leber B, Andrews DW. BH3-only proteins: Orchestrators of apoptosis. Biochim Biophys Acta. 2011;1813:508–20.
4. Singh R, Letai A, Sarosiek K. Regulation of apoptosis in health and disease: the balancing act of BCL-2 family proteins. Nat Rev Mol Cell Biol. 2019;20:175–93.
5. Hanahan D. Hallmarks of cancer: new dimensions. Cancer Discov. 2022;12:31–46.
6. Warren CFA, Wong-Brown MW, Bowden NA. BCL-2 family isoforms in apoptosis and cancer. Cell Death Dis. 2019;10:177.
7. Ashkenazi A, Fairbrother WJ, Leverson JD, Souers AJ. From basic apoptosis discoveries to advanced selective BCL-2 family inhibitors. Nat Rev Drug Discov. 2017;16:273–84.
8. Casara P, Davidson J, Claperon A, Le Toumelin-Braizat G, Vogler M, Bruno A, et al. S55746 is a novel orally active BCL-2 selective and potent inhibitor that impairs hematological tumor growth. Oncotarget. 2018;9:20075–88.
9. Diepstraten ST, Anderson MA, Czabotar PE, Lessene G, Strasser A, Kelly GL. The manipulation of apoptosis for cancer therapy using BH3-mimetic drugs. Nat Rev Cancer. 2022;22:45–64.
10. Konopleva M, Contractor R, Tsao T, Samudio I, Ruvolo PP, Kitada S, et al. Mechanisms of apoptosis sensitivity and resistance to the BH3 mimetic ABT-737 in acute myeloid leukemia. Cancer Cell. 2006;10:375–88.
11. Luo Q, Pan W, Zhou S, Wang G, Yi H, Zhang L, et al. A novel BCL-2 inhibitor APG-2575 exerts synthetic lethality with BTK or MDM2-p53 inhibitor in diffuse large B-cell lymphoma. Oncol Res. 2020;28:331–44.
12. Oltersdorf T, Elmore SW, Shoemaker AR, Armstrong RC, Augeri DJ, Belli BA, et al. An inhibitor of Bcl-2 family proteins induces regression of solid tumours. Nature. 2005;435:677–81.
13. Souers AJ, Leverson JD, Boghaert ER, Ackler SL, Catron ND, Chen J, et al. ABT-199, a potent and selective BCL-2 inhibitor, achieves antitumor activity while sparing platelets. Nat Med. 2013;19:202–8.
14. Tse C, Shoemaker AR, Adickes J, Anderson MG, Chen J, Jin S, et al. ABT-263: A potent and orally bioavailable Bcl-2 family inhibitor. Cancer Res. 2008;68:3421–8.
15. Wilson WH, O'Connor OA, Czuczman MS, LaCasce AS, Gerecitano JF, Leonard JP, et al. Navitoclax, a targeted high-affinity inhibitor of BCL-2, in lymphoid malignancies: a phase 1 dose-escalation study of safety, pharmacokinetics, pharmacodynamics, and antitumour activity. Lancet Oncol. 2010;11:1149–59.
16. Mason KD, Carpinelli MR, Fletcher JI, Collinge JE, Hilton AA, Ellis S, et al. Programmed anuclear cell death delimits platelet life span. Cell. 2007;128:1173–86.
17. Rong YP, Barr P, Yee VC, Distelhorst CW. Targeting Bcl-2 based on the interaction of its BH4 domain with the inositol 1,4,5-trisphosphate receptor. Biochim Biophys Acta. 2009;1793:971–8.
18. Rong YP, Bultynck G, Aromolaran AS, Zhong F, Parys JB, De Smedt H, et al. The BH4 domain of Bcl-2 inhibits ER calcium release and apoptosis by binding the regulatory and coupling domain of the IP3 receptor. Proc Natl Acad Sci USA. 2009;106:14397–402.
19. Jin Z, May WS, Gao F, Flagg T, Deng X. Bcl2 suppresses DNA repair by enhancing c-Myc transcriptional activity. J Biol Chem. 2006;281:14446–56.
20. Denis GV, Yu Q, Ma P, Deeds L, Faller DV, Chen CY. Bcl-2, via its BH4 domain, blocks apoptotic signaling mediated by mitochondrial Ras. J Biol Chem. 2003;278:5775–85.
21. Wang HG, Rapp UR, Reed JC. Bcl-2 targets the protein kinase Raf-1 to mitochondria. Cell. 1996;87:629–38.
22. Shimizu S, Konishi A, Kodama T, Tsujimoto Y. BH4 domain of antiapoptotic Bcl-2 family members closes voltage-dependent anion channel and inhibits apoptotic mitochondrial changes and cell death. Proc Natl Acad Sci USA. 2000;97:3100–5.
23. Lin B, Kolluri SK, Lin F, Liu W, Han YH, Cao X, et al. Conversion of Bcl-2 from protector to killer by interaction with nuclear orphan receptor Nur77/TR3. Cell. 2004;116:527–40.
24. Han B, Park D, Li R, Xie M, Owonikoko TK, Zhang G, et al. Small-molecule Bcl2 BH4 antagonist for lung cancer therapy. Cancer Cell. 2015;27:852–63.
25. Zhang H, Nimmer P, Rosenberg SH, Ng SC, Joseph M. Development of a high-throughput fluorescence polarization assay for Bcl-x(L). Anal Biochem. 2002;307:70–5.
26. Lama L, Adura C, Xie W, Tomita D, Kamei T, Kuryavyi V, et al. Development of human cGAS-specific small-molecule inhibitors for repression of dsDNA-triggered interferon expression. Nat Commun. 2019;10:2261.
27. Padilla-Salinas R, Sun L, Anderson R, Yang X, Zhang S, Chen ZJ, et al. Discovery of small-molecule cyclic GMP-AMP synthase inhibitors. J Org Chem. 2020;85:1579–600.
28. Hou H, Yang R, Liu X, Wu X, Zhang S, Chen K, et al. Discovery of triazoloquinoxaline as novel STING agonists via structure-based virtual screening. Bioorg Chem. 2020;100:103958.
29. Ramanjulu JM, Pesiridis GS, Yang J, Concha N, Singhaus R, Zhang SY, et al. Design of amidobenzimidazole STING receptor agonists with systemic activity. Nature. 2018;564:439–43.
30. Guo ZQ, Zheng T, Chen B, Luo C, Ouyang S, Gong S, et al. Small-molecule targeting of E3 ligase adaptor SPOP in kidney cancer. Cancer Cell. 2016;30:474–84.
31. Zhuang M, Calabrese MF, Liu J, Waddell MB, Nourse A, Hammel M, et al. Structures of SPOP-substrate complexes: Insights into molecular architectures of BTB-Cul3 ubiquitin ligases. Mol Cell. 2009;36:39–50.

32. Halgren T. New method for fast and accurate binding-site identification and analysis. Chem Biol Drug Des. 2007;69:146–8.
33. Halgren TA. Identifying and characterizing binding sites and assessing druggability. J Chem Inf Model. 2009;49:377–89.
34. Nayal M, Honig B. On the nature of cavities on protein surfaces: application to the identification of drug-binding sites. Proteins. 2006;63:892–906.
35. Martinou JC, Youle RJ. Mitochondria in apoptosis: Bcl-2 family members and mitochondrial dynamics. Dev Cell. 2011;21:92–101.
36. Davids MS. Targeting BCL-2 in B-cell lymphomas. Blood. 2017;130:1081–8.
37. Dawson SJ, Makretsov N, Blows FM, Driver KE, Provenzano E, Le Quesne J, et al. BCL2 in breast cancer: A favourable prognostic marker across molecular subtypes and independent of adjuvant therapy received. Br J Cancer. 2010; 103:668–75.
38. Parry N, Wheadon H, Copland M. The application of BH3 mimetics in myeloid leukemias. Cell Death Dis. 2021;12:222.
39. Pore MM, Hiltermann TJ, Kruyt FA. Targeting apoptosis pathways in lung cancer. Cancer Lett. 2013;332:359–68.
40. Liu Z, Wild C, Ding Y, Ye N, Chen H, Wold EA, et al. BH4 domain of Bcl-2 as a novel target for cancer therapy. Drug Discov Today. 2016;21:989–96.
41. Peirs S, Matthijssens F, Goossens S, Van de Walle I, Ruggero K, de Bock CE, et al. ABT-199 mediated inhibition of BCL-2 as a novel therapeutic strategy in T-cell acute lymphoblastic leukemia. Blood. 2014;124:3738–47.